Microstructural evolution and mechanical properties of SnAgCu alloys

Olivier Fouassier, Jean-Marc Heintz, J. Chazelas, Pierre-Marie Geffroy, Jean-François Silvain

Microstructural evolution and mechanical properties of SnAgCu alloys

O. Fouassier and J.-M. Heintz
Institut de Chimie de la Matière Condensée de Bordeaux (ICMCB)—CNRS, Université de Bordeaux 1, Avenue du Dr. Albert Schweitzer, F-33608 Pessac, France

J. Chazelas
Thales Airborne Systems, 2 Avenue Gay Lussac, F-78851 Elancourt, France

P.-M. Geffroy and J.-F. Silvain[a)]
Institut de Chimie de la Matière Condensée de Bordeaux (ICMCB)—CNRS, Université de Bordeaux 1, Avenue du Dr. Albert Schweitzer, F-33608 Pessac, France

(Received 6 January 2006; accepted 28 June 2006; published online 29 August 2006)

Lead containing solder paste is now considered as an environmental threat. In order to eliminate this undesirable environmental impact associated to their production, a family of lead-free solder joint, Sn-3.8Ag-0.7Cu, is proposed. Microstructural and mechanical data of this solder joint have been acquired and compared with the most common used SnPb solder paste. The evolution of the microstructure as well as the failure mode and the mechanical properties of SnAgCu solder joint are discussed as a function of strain rate, annealing treatments, and testing temperature. Tensile tests have been performed, at temperatures ranging from −50 to +150 °C, on bulk samples. Changes of the mechanical properties of bulk tested samples are actually correlated with microstructural changes, as shown by transmission electronic microscopy investigations. © *2006 American Institute of Physics*. [DOI: 10.1063/1.2244478]

I. INTRODUCTION

Today, electronic applications require increasing functionality, speed, compactness, and reliability. These demands lead to larger scale component integration and more compact assembly methods. The design of this kind of assemblies is generally limited by a major problem of reliability. Thermally induced stress between the printed circuit board (PCB) and packaged components leads to joint and system failure under the normal temperature cycling conditions of everyday use. As a result the size of electronic components and the scale of integration are limited.

Conventional solder are based on lead-tin eutectic alloy. In many applications, this solder is used at temperatures exceeding 80% of its melting temperature. At such high homologous temperatures (the ratio of the operating temperature to the melting point, both expressed in Kelvin), the fatigue properties of lead-tin solder are relatively poor and the joints are vulnerable when exposed to thermal mismatch stresses.[1–4] A solder which exhibits enhancements of these properties is crucial in avionics and automotive applications where the solder is subjected to many thermal cycles and sustained temperatures of up to 150 °C. The replacement of this solder by a harder alloy, with a higher melting point, might be beneficial in offering enhanced mechanical performance and then could considerably improve product reliability.

Furthermore, the fact that the great majority of solder alloy contains lead is an environmental threat. Lead-free solder based on tin-silver alloys have gained more attention recently in seeking environmentally friendly solder materials.[5–14] The potential of a lead-free base solder alloy (Sn-3.8Ag-0.7Cu) is evaluated in the present work.

Microstructural and mechanical data of this solder joint have been acquired and compared with the most commonly used SnPb solder paste. The purpose of this work was to understand the evolution of the microstructure with the failure mode and mechanical properties of SnAgCu solder joint. Tensile tests have been performed on bulk samples to correlate microstructural evolution with the modification of the mechanical properties of bulk tested samples. Effects of strain rate, annealing treatment, and temperature of testing have been taken into account.

Transmission electron microscopy was used in order to correlate the evolution of the microstructural and nanostructural characteristics with materials testing processes.

II. EXPERIMENT

A. Sample preparation

Solders were prepared from Sn (95.5 wt %), Ag (3.8 wt %), and Cu (0.7 wt %) powder melted in a crucible, cast into a preheated aluminum mould, and rapidly water quenched. Glycerol was used in order to prevent oxidation of the liquid matrix during the elaboration process. The fast cooling process ensures a reproducible microstructure. These samples are called "as cast sample."

B. Microstructure

The evolution of lead-free solder microstructure with thermal treatment (annealing conditions and cooling rate) and with tensile operating temperatures has been studied. For that purpose, each sample was cross sectioned and mechanically polished. For optical microscope observations, samples

[a)]Electronic mail: silvain@icmcb-bordeaux.cnrs.fr

were etched in a solution containing 2 ml of acetic acid, 2 ml of nitric acid, and 16 ml of glycerol. Distribution of the different solder elements (Sn, Ag, and Cu) was determined using electron probe microanalysis (EPMA) with a lateral and depth resolution of about 1 μm.

C. Mechanical characterization

Tensile tests have been performed on bulk solder sample with an Instron 4466 type machine using a 10 kN load cell. The testing temperature ranged between −70 and +250 °C.

For each data point, five-specimens were tested and average values were calculated. All stresses reported in this paper are nominal stresses, i.e., the cross sectional area of a sample, determined from measurements made before testing, is considered as constant.

The influence of the testing speed and sample aging on the tensile properties of the alloy were investigated as well as the effect of testing temperature on maximum tensile stress and elongation at rupture.

D. Transmission electron microscopy (TEM)

Ultramicrotomy was used for the preparation of solder TEM samples. With this technique, uniform thin slides across heterogeneous phases can be prepared. A JEOL 2000 scanning transmission microscope operating at 200 kV was used to analyze the as prepare solder cross sections.

III. RESULTS

A. Microstructural evolution of SnAgCu samples

Sn-3.8Ag-0.7Cu alloy exhibits a ternary eutectic reaction at 217 °C as shown by the ternary SnAgCu phase diagram established at this temperature.[15] Four phases are in equilibrium: β-Sn rich solid solution, Cu_6Sn_5, Ag_3Sn, and a liquid phase. Because of the eutectic composition of the alloy, the liquid phase has to disappear totally at 217 °C leading to a microstructure composed of the following phases: β-Sn, Cu_6Sn_5, and Ag_3Sn. β-Sn corresponds to an ordered tetragonal lattice with $a=b=5.83$ Å, and $c=3.18$ Å, Cu_6Sn_5 corresponds to an ordered hexagonal compact lattice with $a=b=4.19$ Å and $c=5.09$ Å, and Ag_3Sn corresponds to an ordered orthorhombic lattice with $a=5.97$ Å, $b=4.78$ Å, and $c=5.09$ Å.

Optical examination of the as cast solder alloy reveals a eutectic microstructure penetrated by β-Sn dendrites as seen in Fig. 1.

Figure 2 shows the influence of the cooling rate {air cooled [Figs. 2(a2) and 2(b2)] or water quenched [Figs. 2(a1) and 2(b1)]} on the solder morphology. The slow cooling rate leads to needlelike morphology for the Ag_3Sn and Cu_6Sn_5 precipitates and to the disappearance of the Sn dendrites. These two intermetallics are randomly distributed inside the Sn matrix. This typical microstructure consists of primary tin rich dendrites [dark part in Figs. 2(a1) and 2(b1)] in a near ternary Sn–Ag–Cu eutectic matrix. Silver [white dots in Fig. 2(a1)] and copper [white dots in Fig. 2(b1)] tin compounds are homogeneously distributed in the eutectic phase.

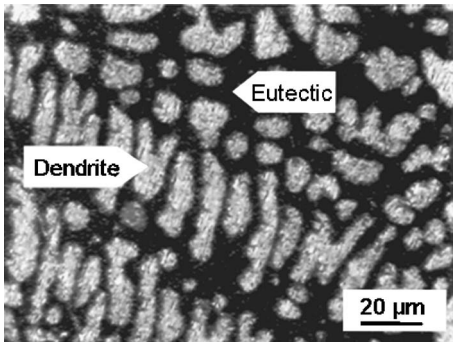

FIG. 1. Optical micrograph of as cast solder.

TEM micrograph of a eutectic area is presented in Fig. 3. Small precipitates ($\phi \leqslant 200$ nm) [Fig. 3(a)] are observed in the tin matrix and were identified to have a composition of Cu_6Sn_5 phase by using energy dispersion x-ray spectrometry (EDX) analysis. It has to be noticed that these precipitates are mainly distributed in Sn grains. Large Ag_3Sn precipitates ($\phi \geqslant 1$ μm) have also been found by TEM investigations [Fig. 3(b)].

Particular attention has been paid to the effect of annealing on the solder microstructure (cf. Fig. 4). To investigate the evolution with temperature and time of the solder microstructure, specimens were annealed at 125 °C under controlled atmosphere for 1, 2, 5, and 600 h. EPMA was performed to assess Sn, Ag, and Cu distributions in the matrix after different annealing treatments. Cu and Ag are homogeneously distributed for short annealing time [Figs. 4(a1) and 4(b1)]. When the annealing time increased it was observed that both Cu–Sn and Ag–Sn precipitates grow. The number of Cu_6Sn_5 precipitate increased and they were mainly located near the tin rich zone interface. It has to be mentioned that for the longer annealing time (600 h at 125 °C) the size and the shape of both precipitates ranged between 1 and 3 μm and that that shape is mostly spherical. The Sn dendrites are quite stable and still present.

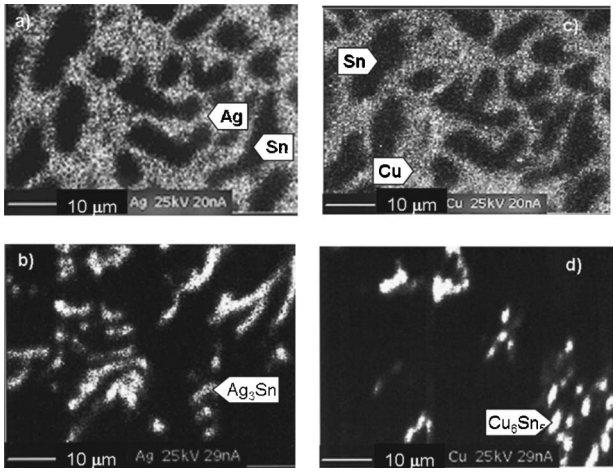

FIG. 2. Ag x-ray mapping solder of (a) rapidly cooled sample (100 °C/min) and (b) slowly cooled sample (1 °C/min). Cu x-ray mapping solder of (c) rapidly cooled sample (100 °C/min) and (d) slowly cooled sample (1 °C/min).

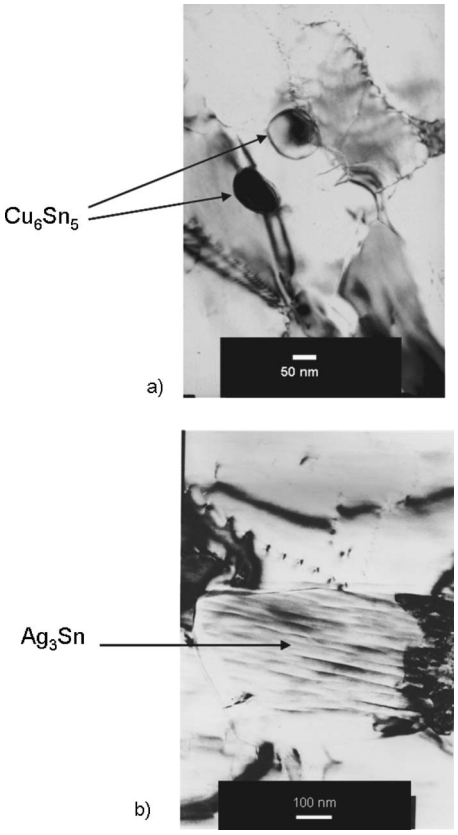

FIG. 3. Transmission electron micrograph of typical intermetallic precipitates observed inside the eutectic region of as cast solder. (a) Cu_6Sn_5 precipitate and (b) Ag_3Sn precipitate.

B. Mechanical properties and corresponding microstructure

Figure 5 shows stress-strain curve for the Sn-3.8Ag-0.7Cu alloy tested in tension at room temperature. The lead-free solder is stiffer than the classical SnPb solder, with a Young's modulus of 50 GPa compared to 32 GPa for SnPb matrix. A very small elastic domain with a yield stress of 29 MPa is observed for the lead-free solder. This value is higher than the SnPb one. Plasticity occurred for strain much lower (0.06%) than the normal elastic strain limit for common metals (0.2%).

1. Influence of the testing speed on the mechanical behavior of the alloy

Tensile tests were performed using four crosshead speeds ranging from 0.5 to 50 mm min^{-1}. These crosshead speeds correspond to strain rates ranging from 2.4×10^{-4} to 2.4×10^{-2} s^{-1} and it agreed with those encountered in solder joint. These tests were carried out at ambient temperature (nominally 20 °C).

Figure 6 shows the evolution of tensile strength with the logarithm of the crosshead speed. A linear relationship is observed. It has to be noticed that the effect of testing speed on strength is much more pronounced for the 60Sn-40Pb alloy[16] but our SnAgCu alloy exhibits higher mechanical strength for every testing speed. Maximum tensile strengths ranging from 45 to 53 MPa were observed.

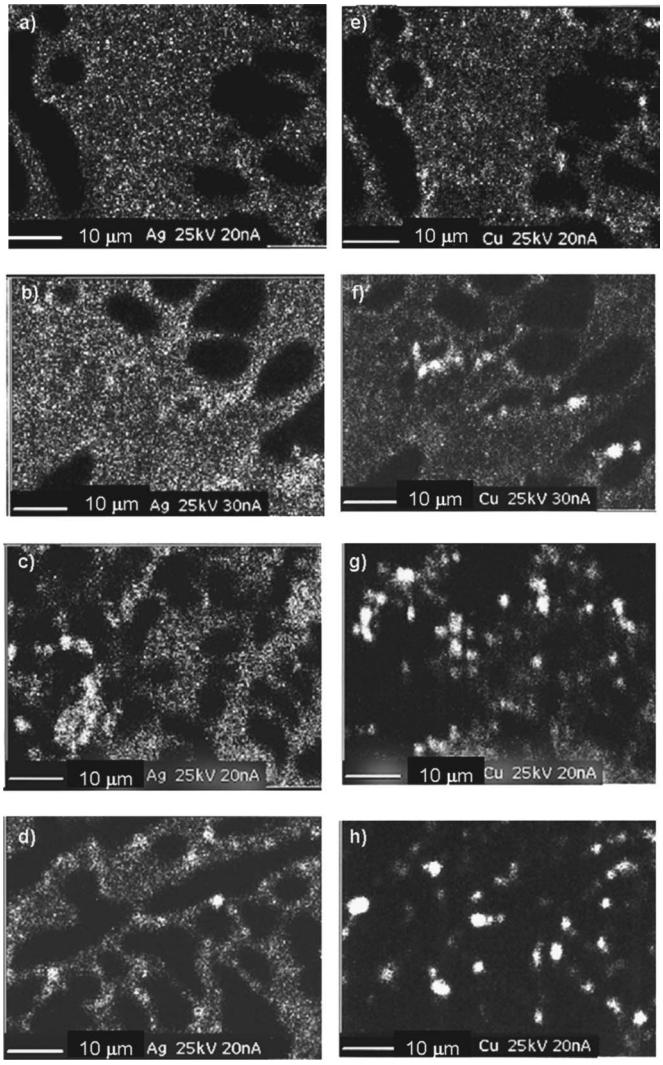

FIG. 4. Ag x-ray mapping solder of slowly cooled sample annealed (a) 1 h, and (b) 2 h, (c) 5 h, and (d) 600 h at 125 °C. Cu x-ray mapping solder of slowly cooled sample annealed (e) 1 h, (f) 2 h, (g) 5 h, and (h) 600 h at 125 °C.

Table I shows the evolution of the maximum tensile stress and elongation at rupture versus crosshead speed for the Sn-3.8Ag-0.7Cu and SnPb matrices. It can be noticed that average elongation at rupture is quasiconstant for the Sn-3.8Ag-0.7Cu matrix (around 20%) but not for the SnPb one.

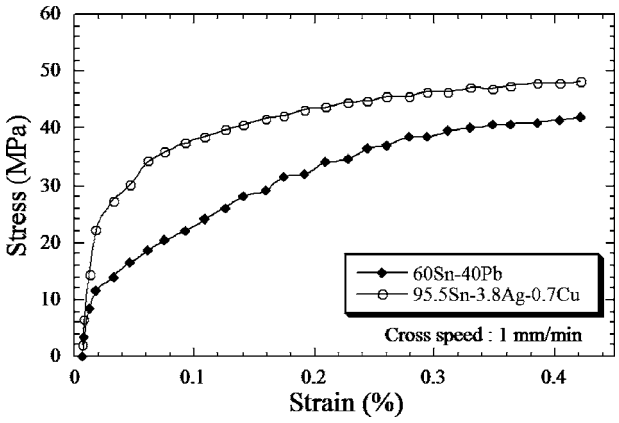

FIG. 5. Stress-strain curve for Sn-3.8Ag-0.7Cu and SnPb.

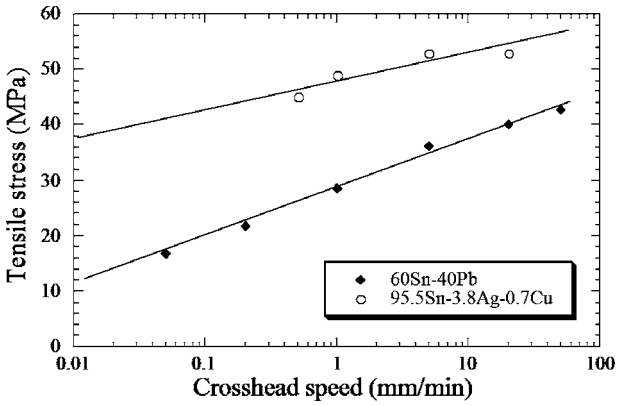

FIG. 6. Tensile strength vs logarithm of crosshead speed.

2. Influence of the annealing temperature on the mechanical behavior of the alloy

Due to the wide range of temperature to which solders are exposed in service conditions, the behavior of the SnAgCu matrix between −50 and 150 °C was studied. Tests were conducted at −50, 20, 50, 100, and 150 °C on as cast specimens. Samples were kept, at testing temperature, 30 min before each tensile test in order to assure a homogeneous temperature distribution inside bulk samples. Maximum tensile stress and elongation at rupture are given in Table II. Several features can be observed: the maximum stress decreases when the temperature increases, and the elongation at rupture increases when testing temperature increases.

3. Influence of the annealing time on the mechanical behavior of the alloy

To correlate mechanical properties with microstructural observations, tensile tests were carried out on specimens heat treated at 125 °C for various annealing times.

Results showed both a decrease in maximum stress and an increase of the rupture strain (Table III). A 22% reduction in strength was found after 1 h annealing. Subsequent annealing leads to slight strength differences. After 600 h of annealing, the total strength decrease was around 40%.

4. Microstructural characterization on tensile tested samples

After rupture of tensile specimens, TEM samples have been prepared near the rupture zone and far away from this zone. Two types of samples subjected to different strain intensities are thus obtained. On these samples, TEM studies have been performed in order to follow the evolution of the solder microstructure and the microstructure and the precipitates characteristics according to the magnitude of the applied stresses.

At −50 °C tested temperature, the main observed difference was related to grain size. Indeed, near the rupture zone, grain size is larger (several microns diameter) compared to areas far away from the rupture zone (diameter ranging from 0.1 to 0.5 μm). It also has to be noticed that an increase of dislocation density can be observed in the larger grain size area. Spherical Cu_6Sn_5 precipitates (diameter around 100 nm) and elongated precipitates (size equal or greater than 1 μm) can be observed all over the testing sample.

For tested temperature ranging from 20 to 100 °C, both large and small grain size associated to high dislocation density and intermetallic precipitates can also be observed near and far from the rupture zone. Nevertheless, it has to be noticed that the percentage of the large grain area increased with annealing temperature, the percentage of the small grain near the rupture zone is higher than the percentage of the large one, and Cu_6Sn_5 and Ag_3Sn precipitates did not grow with the tested temperature. At 150 °C tested temperature, no significant difference in grain size was observed near and far from the rupture zone. However, differences related to intermetallic precipitates were noticed.

Near the rupture zone [Fig. 7(a)], needlelike shape precipitates with thickness around 100–200 nm and lengths of 2 μm and more were observed. Electron diffraction patterns of these precipitates were indexed as an Ag_4Sn phase. This phase corresponds to an ordered hexagonal compact lattice with $a=b=2.97$ Å and $c=4.78$ Å. The appearance of this phase is peculiar and was not observed for other studied samples.

Far from the rupture zone [Fig. 7(b)], Cu_6Sn_5 precipitates are observed in the tin matrix. It has to be mentioned that most of these precipitates are located along grain boundaries. No needlelike shape Ag_4Sn precipitates were observed and no differences in the Sn grain size near and far from the rupture zone were shown.

TABLE I. Evolution of mechanical properties versus crosshead speed. Bold: tensile stress (MPa); italic: elongation at rupture (%).

	Crosshead speed (mm/min)									
	0.5		1		5		20		50	
SnAgCu	**45**	*20*	**50**	*20*	**53**	*21*	**53**	*22*	···	···
SnPb	···	*135*	**28**	···	**36**	···	**40**	···	**42**	*25*

TABLE II. Evolution of mechanical properties as a function of annealing treatment at 125 °C. Crosshead speed: 1 mm/min. Bold: tensile stress (MPa); italic: elongation at rupture (%).

	Testing temperature (°C)									
	−50		20		50		100		150	
SnAgCu	**72**	*16*	**50**	*20*	**35**	*22*	**20**	*22*	**12**	*25*

TABLE III. Evolution of mechanical properties as a function of testing temperature. Crosshead speed: 1 mm/min. Bold: tensile stress (MPa); italic: elongation at rupture (%).

	Annealing treatment at 125 °C									
	As cast		1 h		2 h		5 h		24 h		1000 h	
SnAgCu	**50**	*20*	**38**	*22*	**38**	*23*	**35**	*29*	**34**	*28*	**30**	*27*

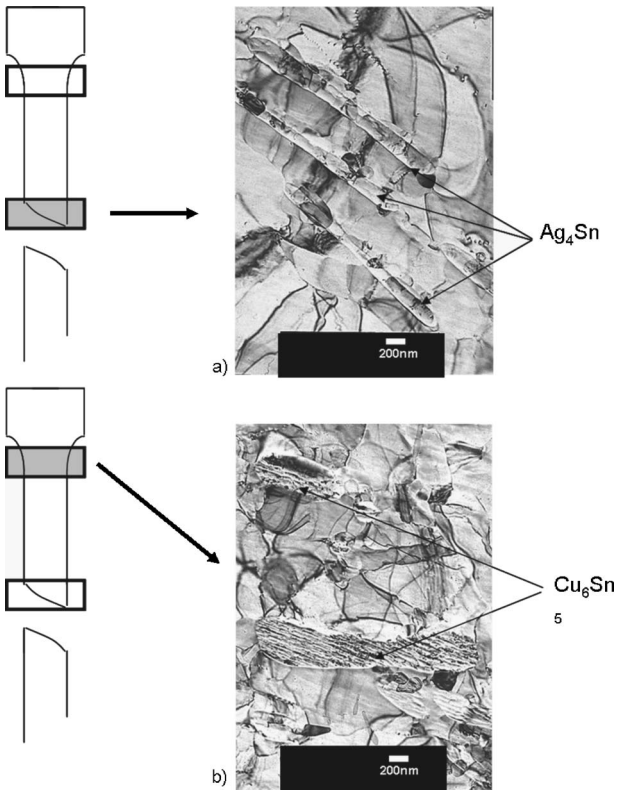

FIG. 7. Transmission electron micrograph of solder samples tested at 150 °C (a) near and (b) far away from the rupture zone.

5. Microstructural characterization on annealed samples

Microstructural studies were also performed to determine the influence of aging on microstructural evolution and more particularly on precipitate growth. A typical TEM micrograph of new precipitate appearing in the sample annealed 600 h at 125 °C is shown in Fig. 8. For this new precipitate morphology, three different zones are observed: (1) A round shape Cu_6Sn_5 precipitates with diameter around 700 nm, (2) a 1.2-μm-thick region containing Ag_4Sn [close to region 1 (Cu_6Sn_5)] and Ag_3Sn [close to region 3 (Sn)] precipitates, and (3) The Sn matrix.

IV. DISCUSSION

Several points arising from this study dealing with the microstructural behavior and the corresponding mechanical properties of annealed and nonannealed Sn-3.8Ag-0.7Cu solder paste matrices are now discussed.

First of all, the microstructure of nonannealed SnAgCu samples is considered. Taking into account the isothermal section of the Sn–Ag–Cu ternary diagram calculated by Moon *et al.*,[17] the reactions that can take place during cooling are the following:

(1) Initial reaction (223–219 °C),

$$L \rightarrow Ag_3Sn + L;$$

(2) monovariant reaction (219–217 °C),

$$Ag_3Sn + L \rightarrow \beta Sn + Ag_3Sn + L;$$

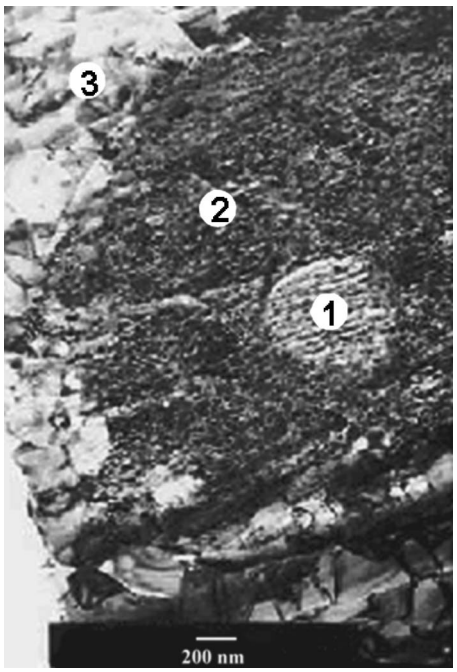

FIG. 8. Transmission electron micrograph of solder sample annealed 1000 h at 125 °C.

(3) eutectic reaction (217 °C),

$$\beta Sn + Ag_3Sn + L \rightarrow \beta Sn + Ag_3Sn + Cu_6Sn_5.$$

Therefore, for an as cast sample, a schematic representation of a slide of the ternary Sn–Ag–Cu is proposed (Fig. 9). From this representation, one can show that a slight change of the Cu and Ag concentration can drastically change the solidification process and therefore the microstructure. Taking into account this representation and our experimental results, the following solidification sequence, for the Sn-

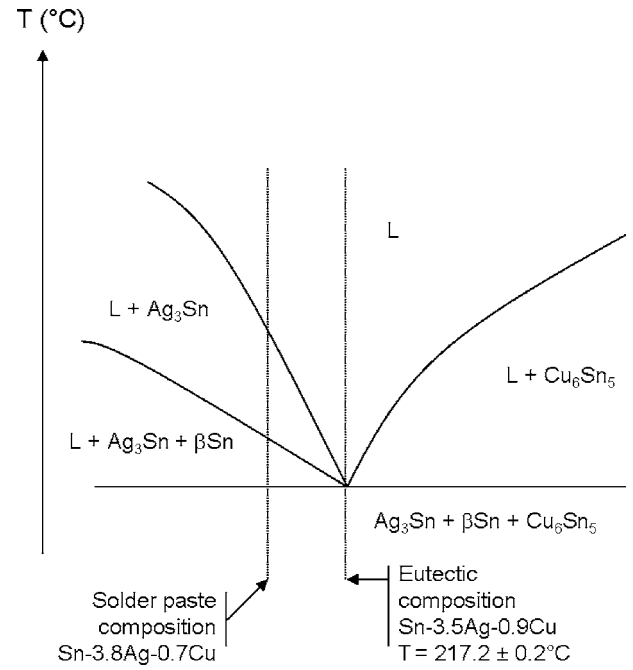

FIG. 9. Schematic representation of a Sn–Ag–Cu ternary slide diagram near the eutectic composition.

3.8Ag-0.7Cu solder paste matrices, is proposed:

(1) Primary precipitation and growth of Ag_3Sn in form of large plates or needles. It has to be noticed that these intermetallic precipitates are much larger (several tens of microns) than those find inside the eutectic structure [close to 1 μm (see Fig. 3)].
(2) $L \rightarrow$ Precipitation of β-Sn in form of either primary dendrite within the liquid or around the above mentioned Ag_3Sn grains.
(3) $L \rightarrow Ag_3Sn + (\beta\text{-Sn})$: binary eutectic reaction.
(4) $L \rightarrow Ag_3Sn + (\beta\text{-Sn}) + Cu_6Sn_5$: ternary eutectic reaction.

The main features concerning the microstructure evolution observed during annealing of the SnAgCu solder paste are the following:

On one hand, the dendritic β-Sn microstructure remains very stable. Indeed no significant evolution of this microstructure has been observed upon annealing up to 600 h at 125 °C.

On the other hand, segregation of copper and silver within the eutectic microstructure occurs. It leads to the formation of larger and more spherical Ag_3Sn and Cu_6Sn_5 intermetallic precipitates. In addition these precipitates are more homogeneously distributed inside the eutectic area for long time annealing.

This behavior can be explained taking into account surface energy minimization phenomena. As a matter of fact, sizes of the β-Sn dendrites ($\sim$tens of microns) are large enough to be stable against annealing time: low surface over volume ratio and large curvature radius. Conversely, the eutectic microstructure is much finer, resulting in a significant surface energy contribution. Therefore, solid state diffusion processes such as Ostwald ripening which is known to lead to particle growth and spheroidization can achieve minimization of this excess surface energy.

Another important feature about microstructure evolutions deals with the growth of Ag_4Sn intermetallic particles for long time annealing (600 h at 125 °C, Fig. 8) or during mechanical testing at 150 °C [near the rupture zone, Fig. 7(a)]. The presence of such a phase is unusual for SnAgCu alloy with compositions close to the ternary eutectic one. In fact, it can be related to the previous mentioned copper diffusion phenomenon that takes place from Cu_6Sn_5 precipitates towards Ag_3Sn in the eutectic microstructure. According to the Sn–Ag–Cu phase diagram studied by Moon *et al.*,[17] an increase of the copper content to Ag_3Sn would result in the formation of a $Ag_3Sn + Ag_4Sn + Cu_3Sn$ phase mixture. Therefore, if copper diffusion is faster than that of silver, Ag_4Sn would actually form at the interface between the two precipitates. Moreover, the needle shape of these precipitates is also in agreement with this phenomenon. Since most of the Ag_3Sn are located at grains boundaries where diffusion processes are more active than in volume, growth of acicular Ag_4Sn along these interfaces is very likely. Formation of these needles during mechanical testing only near the rupture zone shows that this process may also be mechanically activated due to the presence of stress gradients in that zone.

Considering the evolution of the mechanical properties of SnAgCu materials with annealing and testing temperatures, two effects, at least, should be considered: (i) the effect of the annealing time at 125 °C, on the microstructure prior to the tensile test (grain growth, intermetallic growth), and (ii) the effect of the temperature during the tensile test (dislocation mobility, intergranular, and transgranular diffusion phenomena). A coupling of these two effects can obviously append leading to more difficult interpretation of the final mechanical properties of the SnAgCu material.

A. Effect of the annealing time on the microstructure prior to the tensile test

As a first point, it is quite difficult to attribute both the decrease of the maximum tensile stress (MTS) and the increase of elongation at rupture ($A\%$) with annealing temperature to grain growth, as it has been shown by Guy for an annealed Cu–Zn material.[18] Measurement of grain size in such materials is quite difficult. No chemical solution is able to reveal Sn grains. TEM studies can give indications (it seems that some grain growth occurs in our material) but the number of measured grains is too small to give precise values.

B. Effect of the annealing

Secondly, the influence of the crosshead testing speed on the maximum stress and the elongation at rupture has been shown. A classical effect is observed: for a given deformation, an increase of the maximum stress is associated with an increase of the deformation speed. It can be attributed to a viscoplastic behavior of the SnAgCu matrix. In our experiments, the maximum stress increased from 45 to 53 MPa when the deformation speed rose from 2.4×10^{-4} to 9.5×10^{-3} mm/min. These values are comparable to the values obtained by Kariya and Otsuka[19] for a Sn-3.5Ag-1Cu matrix (50 MPa, 5×10^{-3} mm/min).

Now, considering the evolution of the mechanical properties of SnAgCu materials with the annealing and testing temperature two effects, at least, have to be considered: (i) the effect of the annealing temperature, on the microstructure, prior to the tensile test (grain growth and intermetallic growth) and (ii) the effect of the temperature during the tensile test (dislocation mobility and intergranular and transgranular diffusion phenomena). A coupling of these two effects can obviously append leading to more difficult interpretations of the final mechanical properties of the SnAgCu materials.

C. Effect of the annealing temperature, on the microstructure, prior to the tensile test

First of all, the plot of the elongation at rupture ($A\%$) and the tensile stress (TS) (cf. Table III) versus the testing temperature shows a linear increase for $A\%$ together with a decrease of TS. It has been very difficult to correlate this behavior with grain growth as it has previously shown by Guy.[18] Thus, even if TEM studies have shown, for our materials, grain growth after annealing, the small number of grains observed by this technique does not allow us to give precise values of grain size. It has also to be mentioned that

no chemical solutions able to reveal SnAgCu grain size are known. No evidence of recrystallization temperature can be found for the tested samples.

In a second point, EPMA experiments have shown that, during annealing at 125 °C both Ag_3Sn and Cu_6Sn_5 precipitates tend to nucleate and grow leading, after long annealing time, to a stable final configuration where both intermetallics are homogeneously distributed inside the Sn matrix. The driving force for that transformation is a change of temperature which causes the matrix to become unstable. The extent of transformation can be described using the Avrami equation,

$$y = 1 - \exp(-kt^n),$$

where y is the fractional completion of transformation, k is a rate constant, and n is a constant that depends on the mode of transformation. In that equation, it is assumed that the reaction is isothermal and that nucleation takes place prior to the reaction. In our experiments, the mode of transformation can be attributed to a diffusion-controlled transformation with $n = 1.5$. Therefore, diffusion phenomena of copper and silver and growth of intermetallic precipitates are correlated with the annealing temperature: diffusion along long short circuit (grain boundaries, twin) for low temperature and volume diffusion for higher temperature. For the highest temperature (150 °C) TEM analysis have shown that the intermetallic precipitates tend to nucleate along the grain boundaries, therefore diffusion along the long short circuit tends to be more important than volume diffusion.

In a third point, it has to be mentioned that two allotropic tin structures are known in the literature.[20] The β-Sn (quadratic structure) form exists for temperatures greater than 13.2 °C and the α one (cubic structure) for lower temperature (maximum transformation speed around −30 °C). This β to α transformation is associated with a 25% volume increase and therefore a possible destruction of the material (Sn "peste"). In our experiments we did not notice that there was weakening phenomena for the mechanical testing at −50 °C. Therefore, tin should remain in the β structure for all tested temperature.

During testing, the growth of the intermetallic precipitate may be affected by some interactions between the apply load and the material due to differences in crystallographic parameters and elasticity constant between the tin matrix and the Ag_3Sn and Cu_6Sn_5 precipitates.

In summary, during annealing both Sn grains growth and Ag_3Sn and Cu_6Sn_5 intermetallic nucleation and growth occur. The first phenomenon tends to increase the $A\%$ and therefore decrease the TS whereas the second one tends to increase the TS and therefore decrease the $A\%$.

D. Effect of the temperature during the tensile test

Solder materials undergo very complex behavior in response to temperature mainly due to change in microstructure versus external conditions. It is well known that thermal activation plays a significant role during deformation. An increase of temperature favors the slip and/or cross slip of dislocations. Formation of vacancies, which promote climb of dislocations or creep either by diffusion along the grain boundaries (Coble creep) or within the grains (Heering-Nabarro creep), is also temperature dependent, as well as restoration and recrystallization of materials. It is then expected that metallic material can have smaller flow stress and larger rupture strain when temperature increases. This is what was observed for this alloy. Nevertheless it has to be noticed that, whatever the temperature of testing, flow stresses are higher for the lead-free solder compared to the classical SnPb solder. This behavior can be correlated with the higher melting point of the lead-free solder in comparison with the SnPb one.

V. CONCLUSION

The study of Sn-3.8Ag-0.7Cu solders for different cooling conditions and annealing time has shown that the microstructure is highly correlated with the elaboration process. From EPMA studies, it can be seen that as cast and water quenched samples show a dendritic Sn morphology associated with eutectic regions where intermetallics Cu_6Sn_5 and Ag_3Sn particles are finely dispersed within a Sn matrix. For long annealing time and air cooled samples Ag_3Sn and Cu_6Sn_5 precipitates grow with different size and shape.

The evolution of tensile properties of bulk Sn-3.8Ag-0.7Cu samples have been followed with crosshead speed testing (test performed at room temperature), annealing temperature and time (test performed at room temperature), and testing temperature.

It is observed that strength is a function of strain rate, temperature, and annealing treatments. In general, whatever the temperature, an increase in strain rate leads to substantial improvement of the strength and elongation rates. In parallel, whatever the strain rate, an increase in temperature is associated with a decrease of the strength and an increase of the elongation. Furthermore, it has been shown that an increase in ductility is associated with an increase in annealing time. This can be correlated with the homogenization in microstructure observed for long annealing time.

These evolutions of the tensile properties of the bulk Sn-3.8Ag-0.7Cu samples have to be correlated, in some way, with the microstructure evolution of the material. TEM investigations have shown that an increase of the testing temperature is associated with a coarsening of Sn grain size. Depending on the strain intensity to which sample is submitted, different microstructures have been observed. The main result is the formation at 150 °C of Ag_4Sn precipitates near the rupture zone. While a fine dispersion of Ag_3Sn precipitates in the matrix tends to strengthen the material, it is expected that the formation of these Ag_4Sn precipitates with needlelike shape tend to weaken the material. In fact these precipitates, which are certainly brittle, may initiate crack due to their size and shape. This may explain the decrease in strength observed for samples tested at 150 °C.

Finally, Sn-3.8Ag-0.7Cu solder produces stronger bulk material than the classical SnPb solder and as a consequence seems to be a good candidate for the replacement of SnPb solder.

ACKNOWLEDGMENT

The authors thank the European community (BRPR-CT98-0683) for supporting this project.

[1]W. J. Plumbridge, J. Mater. Sci. **31**, 2501 (1996).
[2]W. J. Tomlinson and A. Fullylove, J. Mater. Sci. **27**, 5777 (1992).
[3]J. W. Morris, D. Grivas, D. Tribula, T. Summers, and D. Frear, Soldering Surf. Mount Technol. **4**, 139 (1995).
[4]K. R. Stone, R. Duckett, S. Muckett, and M. Warwick, Brazing & Soldering **4**, 20 (1983).
[5]J. H. Vincent, and G. Humpston, GEC J. Res. **11**, 76 (1994).
[6]J. Glazer, Int. Mater. Rev. **40**, 65 (1995).
[7]S. W. Yoon, C. J. Park, S. H. Hong, J. T. Moon, I. S. Park, and H. S. Chun, J. Electron. Mater. **29**, 1233 (2000).
[8]P. C. Lord, M. C. Witt, R. Bilham, T. Edwards, and C. King, Soldering Surf. Mount Technol. **86**, 173 (1997).
[9]J. C. Foley, A. Gickler, F. H. Leprevost, and D. Brown, J. Electron. Mater. **29**, 1258 (2000).
[10]S. Choi, K. N. Subramanian, J. P. Lucas, and T. R. Bieler, J. Electron. Mater. **29**, 1249 (2000).
[11]W. Yang and R. W. Messler, Jr., J. Electron. Mater. **23**, 765 (1994).
[12]Y. Kariya and M. Otsuka, J. Electron. Mater. **27**, 1229 (1998).
[13]Y. Kariya, Y. Hirita, and M. Otsuka, J. Electron. Mater. **28**, 1263 (1999).
[14]C. M. Miller, I. E. Anderson, and J. F. Smith, J. Electron. Mater. **23**, 595 (1994).
[15]T. Laine-Ylijoki, H. Steen, and A. Forsten, IEEE Trans. Compon., Packag., Manuf. Technol., Part C **20**, 194 (1997).
[16]International Tin Research Institute Report No. 656, 1986 (unpublished).
[17]K. W. Moon, W. J. Boettinger, U. R. Kattner, F. S. Biancaniello, and C. A. Handwerker, J. Electron. Mater. **29**, 1122 (2000).
[18]*Essentials of Materials Science*, edited by A. G. Guy (McGraw-Hill, New York, 1976), p. 340.
[19]Y. Kariya and M. Otsuka, J. Electron. Mater. **27**, 1229 (1999).
[20]O. Fouassier, Thèse des universités, Université de Bordeaux 1, 2001.